Vacuum polarization in the spacetime of a charged nonlinear black hole

Waldemar Berej* and Jerzy Matyjasek†
Institute of Physics, Maria Curie-Skłodowska University, pl. Marii Curie-Skłodowskiej 1, 20-031 Lublin, Poland
(Received 7 April 2002; published 18 July 2002)

Building on general formulas obtained from the approximate renormalized effective action, the approximate stress-energy tensor of the quantized massive scalar field with arbitrary curvature coupling in the spacetime of a charged black hole that is the solution of the coupled equations of nonlinear electrodynamics and general relativity is constructed and analyzed. It is shown that, in a few limiting cases, the analytical expressions relating the obtained tensor to the general renormalized stress-energy tensor evaluated in the geometry of the Reissner-Nordström black hole can be derived. A detailed numerical analysis with special emphasis put on minimal coupling is presented, and the results are compared with those obtained earlier for a conformally coupled field. Some novel features of the renormalized stress-energy tensor are discussed.

DOI: 10.1103/PhysRevD.66.024022 PACS number(s): 04.70.Dy, 04.62.+v

I. INTRODUCTION

One of the most intriguing open questions in modern theoretical physics is the issue of the final stage of black hole evaporation. Although a definite answer would be possible only with the full machinery of a quantum theory of gravity, some important preliminary results may be obtained in principle within the framework of semiclassical theory. However, as the semiclassical approach cannot be used to describe the evolution of the system in the Planck regime, it can, at best, tell us about the tendency rather than the limit itself. Unfortunately, even this simplified program is hard to execute as the semiclassical Einstein field equations comprise a rather complicated set of nonlinear partial differential equations, and, moreover, the source term—the renormalized stress-energy tensor—should be known for a wide class of nonstatic metrics. It is natural, therefore, that, in order to make the back reaction problem tractable, one should refer to some approximations.

It seems that the most promising approach consists in constructing the approximate stress-energy tensor in the geometry of a static black hole and subsequent computation of the semiclassical corrections to the classical metric. Although evaluated in the static background, such corrections, as was pointed out in Ref. [1], are relevant because they give direct information about the influence of the quantum effects on the temperature of a black hole. Thus far this program, initiated in Ref. [2], has been carried out for massless fields in Schwarzschild spacetime [3–8] and for massive scalar fields with arbitrary curvature coupling in Reissner-Nordström (RN) geometry [1], where, among other things, quantum corrections to the geometry, entropy, and trace anomaly were computed. The most important ingredient of the approach is therefore the renormalized stress-energy tensor of the quantized field propagating in the spacetime of a static black hole constructed in a physically interesting state. However, direct evaluation of this object is rather complicated.

It is believed that the physical content of the theory of quantum fields in curved spacetime is contained in the (renormalized) effective action W_R, a useful quantity allowing evaluation of the stress-energy tensor by means of the standard formula

$$\frac{2}{g^{1/2}}\frac{\delta}{\delta g_{ab}}W_{ren}=\langle T^{ab}\rangle_{ren}. \tag{1}$$

Unfortunately, the effective action is a nonlocal functional of the metric and its exact form is unknown. In the attempts to construct the renormalized stress-energy tensor one is forced, therefore, to employ numerical methods or to accept some approximations.

For quantized massive fields in the large mass limit, i.e., when the Compton length is much smaller than the characteristic radius of curvature, the nonlocal contribution to the effective action can be neglected, and the series expansion in m^{-2} of the renormalized effective action W_R may be constructed with the aid of the DeWitt-Schwinger method [9–11]. Thus the constructed renormalized effective action has the form

$$W_{ren}=\frac{1}{32\pi^2m^2}\int d^4x g^{1/2}\sum_{n=3}^{\infty}\frac{(n-3)!}{(m^2)^{n-2}}[a_n(x,x')], \tag{2}$$

where $[a_n(x,x')]$ is the coincidence limit of the nth Hadamard-Minakshisundaram-DeWitt-Seely (HMDS) coefficient. The coefficients are local, geometrical objects constructed from the curvature tensor and its covariant derivatives of rapidly growing complexity. So far, only the coefficients for $n\leqslant 4$ are known, but it seems the effective action constructed from higher order terms would be intractable in practice, especially in attempts to calculate the stress-energy tensor.

The first nonvanishing term of the effective action constructed for the massive scalar field with arbitrary curvature coupling satisfying

$$(-\Box+\xi R+m^2)\phi=0, \tag{3}$$

*Electronic address: berej@tytan.umcs.lublin.pl
†Electronic address: matyjase@tytan.umcs.lublin.pl, jurek@kft.umcs.lublin.pl

where ξ is the coupling constant and m is the mass of the field, from the coincidence limit of the HMDS coefficient $[a_3]$, is given by [12–14]

$$W^{(1)}_{ren}=\frac{1}{192\pi^2m^2}\int d^4xg^{1/2}\Bigg[\frac{1}{2}\left(\eta^2-\frac{\eta}{15}-\frac{1}{315}\right)R\Box R+\frac{1}{140}R_{pq}\Box R^{pq}-\eta^3R^3+\frac{1}{30}\eta RR_{pq}R^{pq}-\frac{1}{30}\eta RR_{pqab}R^{pqab}$$
$$-\frac{8}{945}R^p_qR^q_aR^a_p+\frac{2}{315}R^{pq}R_{ab}R^a{}_p{}^b{}_q+\frac{1}{1260}R_{pq}R^p{}_{cab}R^{qcab}+\frac{17}{7560}R_{ab}{}^{pq}R_{pq}{}^{cd}R_{cd}{}^{ab}-\frac{1}{270}R^a{}_p{}^b{}_qR^p{}_c{}^q{}_dR^c{}_a{}^d{}_b\Bigg]$$
$$=\frac{1}{192\pi^2m^2}\sum_{i=1}^{10}\alpha_iW_{(i)}, \tag{4}$$

where $\eta=\xi-1/6$ and α_i are numerical coefficients that stand in front of the geometric terms in $W^{(1)}_{ren}$. Differentiating $W^{(1)}_{ren}$ functionally with respect to the metric tensor, one obtains

$$\langle T^{ab}\rangle=\sum_{i=1}^{10}\alpha_i\tilde{T}^{(i)ab}=\frac{1}{96\pi^2m^2g^{1/2}}\sum_{i=1}^{10}\alpha_i\frac{\delta W_{(i)}}{\delta g_{ab}}$$
$$=T^{(0)ab}+\eta T^{(1)ab}+\eta^2T^{(2)ab}+\eta^3T^{(3)ab}, \tag{5}$$

where each $\tilde{T}^{(i)ab}$ is a rather complicated expression constructed from the curvature tensor, its covariant derivatives, and contractions. Such calculations were undertaken in Refs. [15,16], where generic expressions for the first nonvanishing order of the renormalized stress-energy tensor were obtained. They generalize earlier results of Frolov and Zel'nikov for vacuum type-D geometries [11]. One can easily extend this result to the case of spinor and vector fields as the analogous expressions differ only by numerical coefficients α_i.

It should be emphasized, however, that the above assumptions place severe limitations on the domain of validity of the approximation obtained. In particular, it would be meaningless, at least in this formulation, to consider the massless limit of the approach. Therefore, the result, which consists of approximately 100 local geometrical terms, may be used in any spacetime provided the temporal changes of the background geometry are slow and the mass of the field is sufficiently large. Because of the complexity of the tensor thus obtained, it will not be presented here, and for its full form and technical details the reader is referred to [16].

For quantized massive scalar fields with arbitrary curvature coupling in static and spherically symmetric geometries there exists a different method invented by Anderson, Hiscock, and Samuel [17]. Their calculations were based on the WKB approximation of the solutions of the radial equation and summation of the mode functions thus obtained. Both methods are equivalent: to obtain the term proportional to m^{-2} one has to use sixth order WKB, and explicit calculations carried out for the Reissner-Nordström spacetime as well as in wormhole geometries considered in Ref. [18] yielded identical results. Moreover, detailed numerical analyses carried out in Ref. [17] and briefly reported in [1] show that for $mM\gtrsim 2$ (M being the black hole mass) the accuracy of the Schwinger-DeWitt approximation in the Reissner-Nordström geometry is quite good (1% or better).

The geometry of the Reissner-Nordström black hole is singular as $r\to 0$ and there is a natural desire to construct its regular generalizations. It is expected that a good candidate for the source term of the Einstein equations is the (classical) stress-energy tensor of nonlinear electrodynamics. Moreover, the renewal of interest in nonlinear electrodynamics that has been seen recently is motivated by the observation that such theories arose as limiting cases of certain formulations of string theory. Unfortunately, the no go theorem proved in Ref. [19] clearly shows that for Lagrangians $\mathcal{L}(F)$ ($F=F_{ab}F^{ab}$), with the Maxwell weak-field limit there are no spherically symmetric static black hole solutions with a regular center.

Recently, employing the Schwinger-DeWitt approximation we constructed the renormalized stress-energy tensor of the quantized conformally coupled massive scalar field in the spacetime of the electrically charged regular black hole that is an exact solution of the equations of nonlinear electrodynamics and the Einstein field equations. Such a solution was proposed by Ayón-Beato and García (ABG) in Ref. [20]. It should be noted, however, that the ABG line element is not a solution of the standard nonlinear electrodynamics and the effective geometry (i.e., the geometry affecting the photons of the nonlinear theory) is singular. Fortunately, the ABG solution may be reinterpreted as describing a magnetically charged regular solution of the coupled equations of standard nonlinear electrodynamics and gravitation with much more regular behavior of the effective geometry [21]. Moreover, it has been shown recently that it is possible to combine electric and magnetic line elements to obtain a regular electric solution with a magnetic core [22].

For small and intermediate charges as well as at large distances, the geometry of the ABG black hole resembles that of RN; noticeable differences appear near the extremality limits. It is interesting therefore to analyze how the similarities in the metric structure of the ABG and RN black

holes are reflected in the structure of the stress-energy tensors. As for the conformally coupled massive scalar field the linear, quadratic, and cubic terms in η in the stress-energy tensor (5) are absent, it is anticipated that such similarities do occur. Explicit calculations carried out in [16] confirmed this hypothesis and showed that for small values of q the appropriate tensors are essentially indistinguishable, and, as expected, important differences appear near and at the extremality limit.

In this paper we shall extend the results of Ref. [16] and investigate a much more complicated case of arbitrary η with special emphasis put on the minimal coupling. Although the complexity of the approximate stress-energy tensor constructed for the ABG line element prevents its direct examination in practice, it is possible to extract interesting information by expanding $\langle T_a^b \rangle$ into a power series and retaining a few leading terms. We shall show that such analyses can be carried out for small charges, large distances, and in the vicinity of the event horizon of the extremal ABG black hole. Moreover, on general grounds one may easily estimate the role played by $\tilde{T}^{(1)ab}$ and $\tilde{T}^{(3)ab}$. To gain a deeper understanding of the problem, however, we employ numerical calculations.

The paper is organized as follows. In Sec. II the essentials of the ABG black hole geometry that are necessary in further development are briefly described. In Sec. III certain features of the approximate stress-energy tensor of the massive scalar field in the ABG geometry are discussed and compared with the appropriate tensors constructed in the RN geometry. The results of our numerical analyses are presented in Sec. IV, in which we discuss the behavior of the components of $\langle T_a^b \rangle$ in some detail and present it graphically.

II. GEOMETRY

The general Reissner-Nordström solution of the Einstein-Maxwell equations describing a static and spherically symmetric black hole of mass M, electric charge e, and magnetic monopole charge e_m has a remarkably simple form:

$$ds^2 = -A(r)dt^2 + A^{-1}(r)dr^2 + r^2(d\theta^2 + \sin^2\theta d\phi^2), \tag{6}$$

with

$$A(r) = 1 - \frac{2M}{r} + \frac{e^2 + e_m^2}{r^2}. \tag{7}$$

Since the charges enter Eq. (7) as a sum of squares, the metric structure remains unchanged under changes of charges leaving $Q^2 = e^2 + e_m^2$ constant. For $Q^2/M^2 < 1$, the equation $A(r) = 0$ has two positive roots:

$$r_\pm = M \pm \sqrt{M^2 - Q^2}, \tag{8}$$

and the larger one, r_+, determines the location of the event horizon, whereas the smaller, r_-, gives the position of the inner horizon. In the limit $Q^2 = M^2$ the horizons merge at $r = M$ and the black hole degenerates to the extremal one. At $r = 0$ the Reissner-Nordström solution has an irremovable curvature singularity, which, although hidden from an external observer for $Q^2/M^2 \leqslant 1$, remains a somewhat unwanted feature of the solution. The solution for $Q^2 > M^2$ is clearly unphysical.

At least for purely electrical solutions the nonlinear electrodynamics does not remedy the situation. Indeed, consider a realization of the nonlinear electrodynamics with the action functional of the form

$$S = \frac{1}{16\pi} \int d^4x \sqrt{-g}[R - \mathcal{L}(F)], \tag{9}$$

where R is a curvature scalar, $F = F_{ab}F^{ab}$, and $\mathcal{L}(F)$ is an arbitrary function with Maxwell asymptotic in the weak-field limit, i.e., $\mathcal{L}(F) \to F$ and $(d/dF)\mathcal{L}(F) \to 1$ as $F \to 0$. According to a well known theorem [19,21], there are no regular, static, and spherically symmetric solutions of general relativity coupled to nonlinear electrodynamics describing a black hole with nonzero electric charge. However, as was explicitly demonstrated recently by Bronnikov, the adopted hypotheses leave room for appropriate regular solutions with a nonzero *magnetic* charge. In this regard it is interesting to note that, within a different formulation of the nonlinear electrodynamics proposed in [23] (a $\mathcal{P}$ framework according to the nomenclature of Refs. [21,24]) obtained from the standard one (the $\mathcal{F}$ formulation) (9) by means of a Legendre transformation, Ayón-Beato and García constructed a regular black hole solution with a nonzero electric charge and mass [20]. Their solution has the simple form (6), where

$$A(r) = 1 - \frac{2M}{r}\left(1 - \tanh\frac{e^2}{2Mr}\right). \tag{10}$$

Bronnikov also demonstrated that any spherically symmetric solution constructed within the $\mathcal{F}$ framework has its counterpart with the same metric tensor constructed within the $\mathcal{P}$ framework, and therefore the electric solution (6) has a magnetic companion with e replaced by the magnetic charge e_m. Moreover, Burinskii and Hildebrandt proposed recently a regular hybrid model in which electrically and magnetically charged solutions were combined in such a way that the electric field does not extend to the center of the black hole [22].

Although the magnetic and electric ABG solutions are precisely of the type (6) with (10), the geometries affecting photons of the nonlinear theory are different. This is because photons of the nonlinear theory move along null geodesics of the effective metric, and the latter is singular for the electric solution [25–27]. It should be noted, however, that otherwise the physical geometry is regular and well behaved.

Since geometries outside the event horizon are described by the same line element and since we are going to consider neutral scalar field only, our results will hold for any particular realization of the ABG black hole as the only concern here is the metric structure of the spacetime. Therefore in what follows we denote both the electric and magnetic charge by e.

Inspection of the metric potentials reveals interesting features of the ABG solution: its curvature invariants are finite

as $r \to 0$ and at large r it approaches the Reissner-Nordström solution. Moreover, for small and intermediate values of the ratio e^2/M^2, the radial coordinate of the event horizon, r_+, is close to the event horizon of the RN black hole; significant differences occur near the extremality limit.

It was shown in [16] that the location of the horizons of the ABG black hole may be expressed in terms of the Lambert function W [28]. Indeed, making use of the substitution $r=Mx$, $e^2=q^2M^2$, it can be demonstrated that the location of the horizons is given by the real branches of the Lambert functions:

$$x_\pm = -\frac{4q^2}{4W(\varepsilon,-q^2/4\exp(q^2/4))-q^2}, \tag{11}$$

where ε is 0 for the event horizon x_+, and -1 for the inner one x_-. The functions $W(0,s)$ and $W(-1,s)$ are the only real branches of the Lambert function with the branch point at $s=-\mathrm{e}^{-1}$, where e is the base of natural logarithms and

$$W(0,-\mathrm{e}^{-1})=W(-1,-\mathrm{e}^{-1})=-1. \tag{12}$$

Consequently, for

$$q=2\sqrt{w} \tag{13}$$

the horizons merge at

$$x_{extr}=\frac{4w}{1+w}, \tag{14}$$

where $w=W(0,\mathrm{e}^{-1})=0.2785$. Numerically, one has $x_{extr}=0.871$ for $|e|/M=1.055$.

For small values of q, the ABG line element resembles that of RN. Indeed, expanding the function $A(x)$ one has

$$A(x)=1-\frac{2}{x}+\frac{q^2}{x^2}+\mathcal{O}(q^4). \tag{15}$$

In spite of the similarities between the ABG and RN geometries for $q\ll 1$, there are substantial differences in the extremality limit: the extremal RN line element is described by Eq. (6) with

$$A(x)=\left(1-\frac{1}{x}\right)^2, \tag{16}$$

whereas near the event horizon of the extremal ABG black hole the function $A(x)$ has the following expansion:

$$A(x)=\frac{(1+w)^3}{32w^2}(x-x_{extr})^2+\mathcal{O}(x-x_{extr})^3. \tag{17}$$

The form of the above expansion indicates that the proper length between the event horizon and any point located at $r>r_{extr}$ is infinite.

III. THE RENORMALIZED STRESS-ENERGY TENSOR

The structure of terms in the effective potential (4) and in Eq. (5) indicates that for the conformally coupled massive scalar field, i.e., for $\eta=0$, there are substantial simplifications of the renormalized stress-energy tensor, as in this very case the third, fourth, and fifth terms in Eq. (4) do not contribute to the final result. Moreover, from Eq. (4) it is evident that in $R=0$ geometries and for arbitrary curvature coupling the functional derivative of the first and the third terms in Eq. (4) with respect to the metric tensor vanishes and, therefore, the approximate renormalized stress-energy tensor of the massive field in RN spacetime has the general form

$$T_a^b=C_a^b+\eta D_a^b. \tag{18}$$

On the other hand, however, for the ABG metric one has

$$R=\frac{q^4}{M^2x^5}\tanh\left(\frac{q^2}{2x}\right)\left[1-\tanh^2\left(\frac{q^2}{2x}\right)\right], \tag{19}$$

which for small q is $\mathcal{O}(q^6)$. Detailed calculations carried out for $q\ll 1$ show that for the ABG solution neither $\tilde{T}_a^{(1)b}$ nor $\tilde{T}_a^{(3)b}$ contributes importantly to the result.

Because of the similarities of the metric structures of the RN and ABG solutions, the overall behavior of the renormalized stress tensors for conformal coupling should be qualitatively similar and comparable in magnitude at least for small and intermediate values of q. However, the differences between the line element (16) and the expansion (17) give strong evidence for differences in the appropriate components of the approximate stress-energy tensors. For the conformally coupled massive scalar field this statement has been confirmed by the extensive numerical calculations reported in Ref. [16]. Now we shall analyze the case of an arbitrary coupling with curvature. First, observe that the contribution of $\eta^2\tilde{T}^{(1)ab}$ and $\eta^3\tilde{T}^{(3)ab}$ to the stress-energy tensor can be made arbitrarily great by a suitable choice of the conformal coupling. It should be noted, however, that such great values of η are clearly unphysical and should be rejected. Therefore, as the particular case of the conformal coupling was considered earlier, here we shall confine ourselves mostly to the important and physically interesting case of minimal coupling $\eta=-1/6$.

In order to construct C_a^b and D_a^b one has either to calculate the curvature tensor and its covariant derivatives to required order for the line element (6) with (7) and employ the general formulas presented in [15] or to make use of the method proposed by Anderson, Hiscock, and Samuel [17]. Both approaches yield the same result, which reads

$$C_t^t=\frac{810x^4q^2-855x^4-202x^2q^4+1878x^3-1152x^3q^2-2307x^2q^2+3084xq^4-1248q^6}{30240M^6\pi^2m^2x^{12}}, \tag{20}$$

$$D_t^t=\frac{-1008x^3q^2+819q^6+2604x^2q^2+728x^2q^4-2712xq^4+360x^4-792x^3}{720M^6\pi^2m^2x^{12}}, \tag{21}$$

$$C_t^t=\frac{842x^2q^4+444q^6+162x^4q^2-462x^3-1488x^3q^2-1932xq^4+315x^4+2127x^2q^2}{30240M^6\pi^2m^2x^{12}}, \tag{22}$$

$$D_r^r=\frac{504xq^4-208x^2q^4-588x^2q^2+336x^3q^2-117q^6+216x^3-144x^4}{720M^6\pi^2m^2x^{12}}, \tag{23}$$

$$C_\theta^\theta=\frac{2202x^3-486x^4q^2-945x^4-3044x^2q^4+4884x^3q^2-9909x^2q^2+10356xq^4-3066q^6}{30240M^6\pi^2m^2x^{12}}, \tag{24}$$

and

$$D_\theta^\theta=\frac{-1176x^3q^2+1053q^6+3276x^2q^2+832x^2q^4-3408xq^4+432x^4-1008x^3}{720M^6\pi^2m^2x^{12}}. \tag{25}$$

The analogous tensor in the ABG geometry is more complicated, and besides the linear terms it contains also terms that are quadratic and cubic in η. Each component of the stress-energy tensor consists of more than 300 terms and has the general form

$$\frac{1}{96\pi^2m^2M^6}\left(1-\tanh\frac{q^2}{2x}\right)\sum_{i,j,k}\alpha_{ijk}\frac{q^{2i}}{x^j}\tanh^k\frac{q^2}{2x}, \tag{26}$$

where α_{ijk} for a given η are numerical coefficients ($0\leqslant i\leqslant 6$, $8\leqslant j\leqslant 15$, $0\leqslant k\leqslant 8$), and for obvious reasons will not be presented here.

Since the form of Eq. (26) differs considerably from the stress-energy tensor given by Eq. (18) with Eqs. (20)–(25), it could be expected that the runs of both tensors have nothing in common. On the other hand, similarities in the metric structure of the RN and ABG black holes discussed earlier strongly suggest the opposite. Unfortunately, the complexity of the renormalized stress-energy tensor of the massive scalar field in the ABG geometry invalidates direct analytical treatment in practice. One can, however, obtain interesting and important information analyzing certain limiting cases. Indeed, expanding the stress-energy tensor for $q\ll 1$ one has

$$\langle T_a^b\rangle^{ABG}=T_a^b+\Delta_a^{(1)b}+\mathcal{O}(q^8), \tag{27}$$

where T_a^b is given by Eqs. (18)–(25) and

$$96\pi^2m^2\Delta_t^{(1)t}=-\frac{q^6(12049-11416x+2660x^2)}{420M^6x^{12}}+\frac{2q^6(617-596x+140x^2)\eta}{5M^6x^{12}}-\frac{12q^6(459-366x+70x^2)\eta^2}{M^6x^{12}}, \tag{28}$$

$$96\pi^2m^2\Delta_r^{(1)r}=-\frac{q^6(1555-1064x+140x^2)}{420M^6x^{12}}-\frac{2q^6(121-140x+40x^2)\eta}{5M^6x^{12}}+\frac{12q^6(81-84x+20x^2)\eta^2}{M^6x^{12}}, \tag{29}$$

$$96\pi^2m^2\Delta_\theta^{(1)\theta}=\frac{q^6(5249-3528x+560x^2)}{420M^6x^{12}}+\frac{2q^6(779-720x+160x^2)\eta}{5M^6x^{12}}-\frac{12q^6(540-423x+80x^2)\eta^2}{M^6x^{12}}. \tag{30}$$

Inspection of expansions (28)–(30), which are valid for any η and x, shows that in this order the term $\tilde{T}_{(3)}^{ab}$ is absent in the

final result. This is because $\tilde{T}_a^{(3)b}\sim\mathcal{O}(q^{12})$. The second term $\tilde{T}_a^{(1)b}$, which vanishes in the RN geometry, is now $\mathcal{O}(q^6)$.

A similar expansion valid for large values of the radial coordinate has the following form:

$$\langle T_a^b\rangle^{ABG}=T_a^b+\Delta_a^{(1)b}+\Delta_a^{(2)b}+\mathcal{O}(x^{-13}), \tag{31}$$

where T_a^b is given by Eqs. (18)–(25), $\Delta_a^{(1)b}$ by Eqs. (28)–(30), and

$$96\pi^2m^2\Delta_t^{(2)t}=\frac{q^8(-2574+1015q^2)}{210M^6x^{12}}-\frac{14q^8(-39+20q^2)\,\eta}{5M^6x^{12}}+\frac{105q^8(-27+8q^2)\,\eta^2}{M^6x^{12}}, \tag{32}$$

$$96\pi^2m^2\Delta_r^{(2)r}=\frac{q^8(-738+35q^2)}{378M^6x^{12}}+\frac{4q^8(-51+28q^2)\,\eta}{9M^6x^{12}}-\frac{5q^8(-333+112q^2)\,\eta^2}{3M^6x^{12}}, \tag{33}$$

$$96\pi^2m^2\Delta_\theta^{(2)\theta}=\frac{q^8(12456-875q^2)}{1890M^6x^{12}}-\frac{112q^8(-12+5q^2)\,\eta}{9M^6x^{12}}+\frac{5q^8(-1989+560q^2)\,\eta^2}{3M^6x^{12}}. \tag{34}$$

Note that in Eqs. (32)–(34) there is no contribution from the term $\tilde{T}_a^{(3)b}$ and, consequently, the result, which is valid for any combination of couplings and charges, is independent of η^3.

In the vicinity of the event horizon of the extremal black hole the renormalized stress-energy tensor has the following expansion:

$$96\pi^2m^2\langle T_a^b\rangle^{ABG}=t_a^{(1)b}+t_a^{(2)b}(x-x_{extr})+\mathcal{O}(x-x_{extr})^2, \tag{35}$$

$$t_t^{(1)t}=t_r^{(1)r}=-\frac{1}{4096}\frac{(1+w)^6(2+w)(w-1)^2\eta^3}{w^6M^6}-\frac{1}{245760}\frac{(1+w)^6(4+w+w^3+2w^2)\,\eta}{w^6M^6}+\frac{1}{1935360}\frac{(1+w)^6(w^3+3w^2+3w+5)}{w^6M^6}, \tag{36}$$

$$t_t^{(2)t}=t_r^{(2)r}=\frac{3}{16384}\frac{(1+w)^7(w+3)(w^2-2w+1)\,\eta^3}{w^7M^6}-\frac{1}{2580480}\frac{(1+w)^7(w+3)(w^2+3)}{w^7M^6}+\frac{1}{983040}\frac{(1+w)^7(w+3)(3w^2-2w+7)\,\eta}{w^7M^6}, \tag{37}$$

$$t_\theta^{(1)\theta}=t_\phi^{(1)\phi}=\frac{1}{8192}\frac{(1+w)^6(w+5)(w-1)^2\eta^3}{w^6M^6}+\frac{1}{491520}\frac{(1+w)^6(-w+13+3w^2+w^3)\,\eta}{w^6M^6}-\frac{1}{3870720}\frac{(1+w)^6(3w+17+3w^2+w^3)}{w^6M^6}, \tag{38}$$

and

$$t_\theta^{(2)\theta}=t_\phi^{(2)\phi}=-\frac{3}{32768}\frac{(1+w)^7(-25w+34-23w^2+9w^3+5w^4)\,\eta^3}{M^6w^7}-\frac{1}{16384}\frac{(1+w)^7(-10w-8+w^2+4w^3+w^4)\,\eta^2}{M^6w^7}+\frac{1}{1966080}\frac{(1+w)^7(-185w-190-111w^2+5w^4-15w^3)\,\eta}{M^6w^7}. \tag{39}$$

Since $\tilde{T}_a^{(1)b}$ vanishes in the limit $x\to x_{extr}$ there are no terms proportional to η^2 in Eqs. (36)–(38).

The components of the stress-energy tensor of the massive scalar field are regular functions of the radial coordinate and are finite on the event horizon. Moreover, it can be demonstrated that the difference between the radial and time components of $\langle T_a^b \rangle^{ABG}$ factorizes:

$$\langle T_t^t \rangle^{ABG} - \langle T_r^r \rangle^{ABG} = \left[1 - \frac{2M}{r} \left(1 - \tanh \frac{e^2}{2Mr} \right) \right] F(r), \tag{40}$$

where $F(r)$ is a regular function and, consequently, the stress-energy tensor is finite in a freely falling frame. To demonstrate this let us consider a slightly more general line element:

$$ds^2 = -f(x^1)(dx^0)^2 + g(x^1)(dx^1)^2 + (x^1)^2 d\Omega^2. \tag{41}$$

For radial motion the vectors of the frame are the four-velocity $e_0^\alpha = u^\alpha$ and a unit length spacelike vector $e_1^\alpha = n^\alpha$. Then, using the geodesic equation, one finds

$$e^a_{(0)} = u^a = \left(\frac{\gamma}{f}, -\sqrt{\left(\frac{\gamma^2}{f} - 1 \right) \frac{1}{g}}, 0, 0 \right) \tag{42}$$

and

$$e^a_{(1)} = n^a = \left(-\frac{1}{f}\sqrt{\gamma^2 - f}, \frac{\gamma}{\sqrt{fg}}, 0, 0 \right), \tag{43}$$

where γ is the energy per unit mass along the geodesic. A simple calculation shows that the components $T_{(0)(0)}$, $T_{(0)(1)}$, and $T_{(1)(1)}$ in a freely falling frame [independent of the function $g(x^1)$] are

$$T_{(0)(0)} = \frac{\gamma^2 (T_1^1 - T_0^0)}{f} - T_1^1, \tag{44}$$

$$T_{(1)(1)} = \frac{\gamma^2 (T_1^1 - T_0^0)}{f} + T_1^1, \tag{45}$$

$$T_{(0)(1)} = -\frac{\gamma \sqrt{\gamma^2 - f} (T_1^1 - T_0^0)}{f}. \tag{46}$$

One concludes, therefore, that if all components of T_a^b and

$$\frac{(T_1^1 - T_0^0)}{f} \tag{47}$$

are finite on the horizon, the stress-energy tensor in a freely falling frame is finite as well. It is expected that the formulas constructed satisfactorily approximate the exact stress-energy tensor. On the other hand, however, to establish the regularity of the exact $\langle T_a^b \rangle^{ABG}$ in a freely falling frame one has to explicitly demonstrate that Eq. (47) is satisfied.

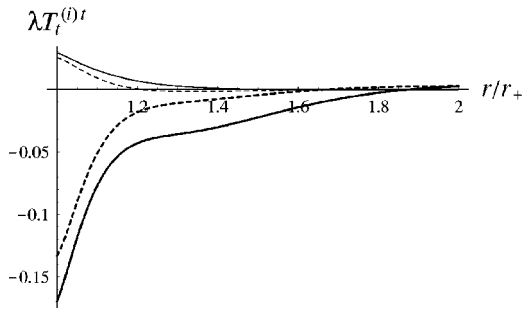

FIG. 1. The radial dependence of the rescaled time component $\lambda T_t^{(1)t}$ ($\lambda = 96\pi^2 M^6 m^2$) (solid thick line) and $\lambda T_t^{(0)t}$ (solid thin line) contributing to the renormalized stress-energy tensor of the massive scalar field for the extremal ABG geometry. The dashed lines correspond to the appropriate tensors for the extremal RN black hole: λC_t^t (thin curve) and λD_t^t (thick curve).

IV. NUMERICAL RESULTS

The considerations of the previous section are limited to analytically tractable special cases. However, to gain insight into the overall behavior of the stress-energy tensor for any combination of couplings and charges one has to refer to numerical calculations—our complete but rather complicated analytical formulas are, unfortunately, not of much help in this regard. Below we describe the main features of the constructed tensors and present them graphically, fixing our attention on the physically interesting case of minimal coupling. Related plots showing the radial dependence of C_a^b and $T_a^{(0)b}$ can be found in Ref. [16], where a discussion of the stress-energy tensor of the massive scalar field with conformal coupling with curvature is presented.

The case of arbitrary η is much more complicated as the tensor $\langle T_a^b \rangle^{ABG}$, given by Eq. (5), is modified by the presence of additional terms. However, numerical analysis performed for $\eta = -1/6$ reveals that the contribution of $\eta^3 T_a^{(3)b}$ is negligible for q even as large as 1.0. Moreover, a closer examination indicates that, as one approaches the extremality limit, the magnitude of this very term becomes comparable with $\eta^2 T_a^{(2)b}$ and $\eta T_a^{(1)b}$ only in the closest vicinity of the event horizon. Our calculations also suggest that, irrespective of

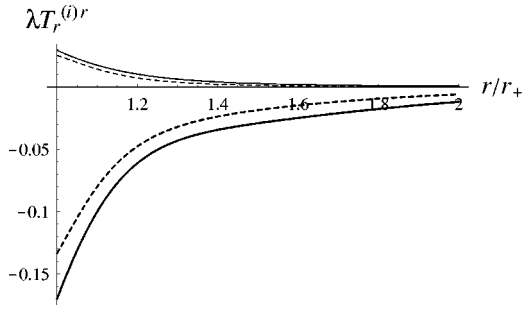

FIG. 2. The radial dependence of the rescaled radial component $\lambda T_r^{(1)r}$ ($\lambda = 96\pi^2 M^6 m^2$) (solid thick line) and $\lambda T_r^{(0)r}$ (solid thin line) contributing to the renormalized stress-energy tensor of the massive scalar field for the extremal ABG geometry. The dashed lines correspond to the appropriate tensors for the extremal RN black hole: λC_r^r (thin curve) and λD_r^r (thick curve).

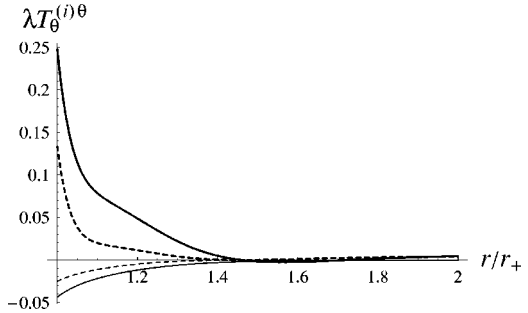

FIG. 3. The radial dependence of the rescaled angular component $\lambda T_\theta^{(1)\theta}$ ($\lambda=96\pi^2M^6m^2$) (solid thick line) and $\lambda T_\theta^{(0)\theta}$ (solid thin line) contributing to the renormalized stress-energy tensor of the massive scalar field for the extremal ABG geometry. The dashed lines correspond to the appropriate tensors for the extremal RN black hole: λC_θ^θ (thin curve) and λD_θ^θ (thick curve).

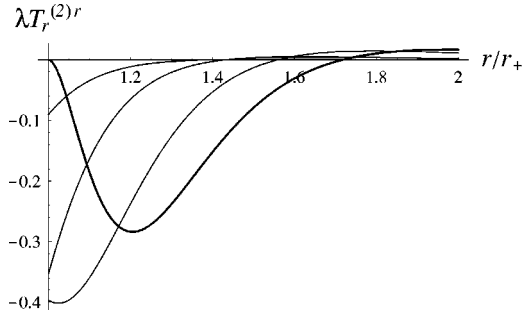

FIG. 5. The radial dependence of the rescaled radial component $\lambda T_r^{(2)r}$ ($\lambda=96\pi^2M^6m^2$) contributing to the renormalized stress-energy tensor of the arbitrarily coupled massive scalar field in the ABG geometry. The thick curve corresponds to the extremal case and the thin curves are for a series of q values approaching the extremality limit, $q=0.9,1,1.05$.

the exact value of q, each component of $T_a^{(1)b}$ is a monotonic function of the radial coordinate in a large neighborhood of the event horizon, if not in the whole range $r>r_+$. For the extremal case such behavior is illustrated in Figs. 1–3, where the time, radial, and angular components of $T_a^{(1)b}$ are displayed. For comparison and completeness we also present the run of $T_a^{(0)b}$, C_a^b, and D_a^b, where the latter two tensors have been calculated for the RN line element with the aid of Eqs. (20)–(25). It should be noted that even in the extremal case, when the differences between the two considered geometries are most prominent, the tensors $T_a^{(1)b}$ and D_a^b behave in a similar manner although differing noticeably in magnitude. For small values of q, the curves constructed for both types of black hole are almost indistinguishable, which can be easily established from Eq. (27).

On the other hand, however, the components of $T_a^{(2)b}$ exhibit quite different but very regular behavior, which will be described in some detail. For $q\ll1$ it can be, of course, inferred from the approximate formulas (27)–(30); greater values of q require numerical examination. Specifically, for small charges each component of the considered tensor is negative at $r=r_+$, and, before approaching zero as $r\to\infty$, it changes sign once for the radial component and twice for time and angular components. With increase of q, all components become strongly negative at r_+, with their zeros shifted toward larger values of the radial coordinate. Near the extremality limit, the tensor $T_a^{(2)b}$ is very sensitive to changes of q, which is illustrated in Figs. 4–6. If the value of the ratio $|e|/M$ slightly exceeds 1.0, for all components there occurs a negative minimum not far away from the event horizon. For the extremal ABG black hole $T_a^{(2)b}$ vanishes at r_+, as is clearly seen from Eqs. (35)–(38), and exhibits oscillatory-like behavior with a rapidly decreased amplitude and increased intervals between zeros. The angular component attains a very distinct maximum near the event horizon whereas for time and radial component there are minima close to r_+.

The competition of the terms described above results in the overall behavior of the stress-energy tensor of minimally coupled massive fields in the geometry of the ABG black hole. Numerical calculations indicate that for small and intermediate values of q, up to about 0.8, $\langle T_a^b\rangle^{ABG}$ still resembles that evaluated for conformal coupling. For larger values of q, however, the change of curvature coupling leads to a considerable modification of the results as both magnitudes and radial variations become significantly different.

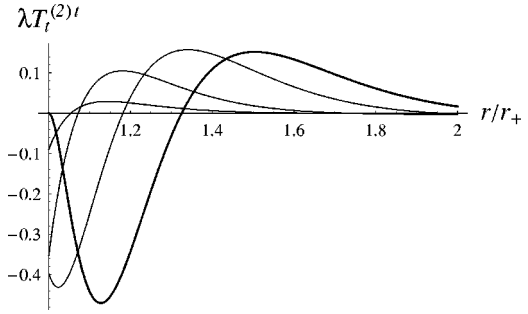

FIG. 4. The radial dependence of the rescaled time component $\lambda T_t^{(2)t}$ ($\lambda=96\pi^2M^6m^2$) contributing to the renormalized stress-energy tensor of the arbitrarily coupled massive scalar field in the ABG geometry. The thick curve corresponds to the extremal case and the thin curves are for a series of q values approaching the extremality limit, $q=0.9,1,1.05$.

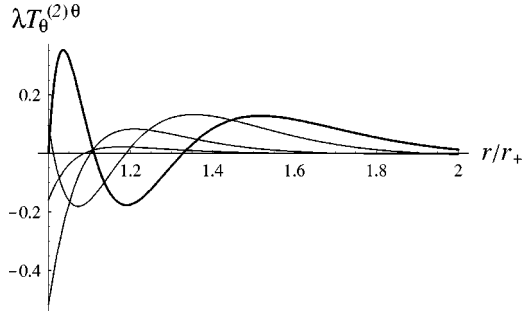

FIG. 6. The radial dependence of the rescaled angular component $\lambda T_\theta^{(2)\theta}$ ($\lambda=96\pi^2M^6m^2$) contributing to the renormalized stress-energy tensor of the arbitrarily coupled massive scalar field in the ABG geometry. The thick curve corresponds to the extremal case and the thin curves are for a series of q values approaching the extremality limit, $q=0.9,1,1.05$.

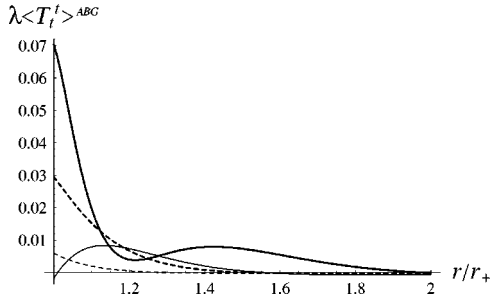

FIG. 7. The radial dependence of the rescaled time component $\lambda\langle T_t^t\rangle^{ABG}$ ($\lambda=96\pi^2M^6m^2$) of the renormalized stress-energy tensor of the minimally coupled massive scalar field in the ABG geometry (solid lines) as compared to the case of conformal coupling in this geometry (dashed lines). The thin curves are for $q=1.02$ and the thick curves are for the extremal case.

This is illustrated in Figs. 7–9, where values of q at and near the extremality limit were chosen. The oscillatory-like behavior of $T_a^{(2)b}$ for q close to q_{extr} is reflected by the presence of local extrema visible in the stress-energy tensor, and, for the angular component, an inflection point. This is in sharp contrast with the almost monotonic behavior of the stress-energy tensor of conformally coupled massive fields depicted in Figs. 7–9 by the dashed lines. Moreover, it should be noted that for $\eta=-1/6$, when the extremality limit is approached, there are substantial changes of values of $\langle T_a^b\rangle^{ABG}$ at the event horizon as well as in the behavior of the stress-energy tensor in a narrow strip near r_{extr}. There appear also certain new features for the time and radial components which are not present in the case of conformal coupling. Indeed, for $0.987\lesssim q\lesssim 1.032$, the energy density $\rho=-\langle T_t^t\rangle^{ABG}$ is positive at the event horizon whereas for the same values of q the horizon value of the radial pressure $p_r=\langle T_r^r\rangle^{ABG}$ is negative. It should be noted in this regard that for $\eta=0$ the radial component of the stress-energy tensor is always positive there. On the other hand, the angular pressure is positive on the event horizon for $|e|/M\lesssim 0.922$ and negative for larger values, which is very similar to the previously studied case of conformal coupling.

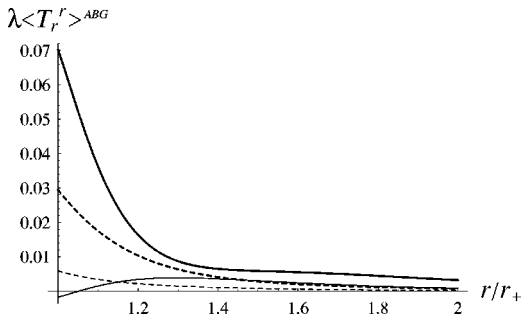

FIG. 8. The radial dependence of the rescaled radial component $\lambda\langle T_r^r\rangle^{ABG}$ ($\lambda=96\pi^2M^6m^2$) of the renormalized stress-energy tensor of the minimally coupled massive scalar field in the ABG geometry (solid lines) as compared to the case of conformal coupling in this geometry (dashed lines). The thin curves are for $q=1.02$ and the thick curves are for the extremal case.

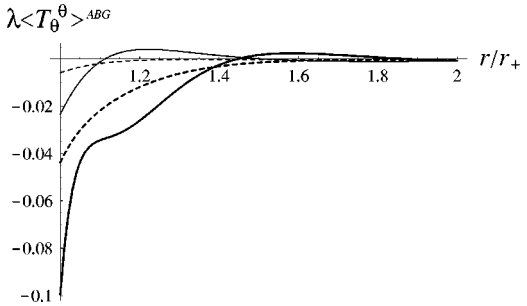

FIG. 9. The radial dependence of the rescaled angular component $\lambda\langle T_\theta^\theta\rangle^{ABG}$ ($\lambda=96\pi^2M^6m^2$) of the renormalized stress-energy tensor of the minimally coupled massive scalar field in the ABG geometry (solid lines) as compared to the case of conformal coupling in this geometry (dashed lines). The thin curves are for $q=1.02$ and the thick curves are for the extremal case.

V. CONCLUDING REMARKS

In this work our goal was to construct the renormalized stress-energy tensor of the quantized massive field in the spacetime of a nonlinear black hole and to investigate how the choice of the curvature coupling affects the results. A regular electrically charged solution of this type was recently proposed by Ayón-Beato and García in the $\mathcal{P}$ formulation of nonlinear electrodynamics and reinterpreted by Bronnikov as a regular magnetically charged solution of the standard $\mathcal{F}$ formulation. For small and intermediate values of the ratio $|e|/M$ the metric structure of the nonlinear solution closely resembles that of Reissner and Nordström and the similarities in the line elements are reflected in the behavior of the stress-energy tensor of the conformally coupled massive scalar fields; notable differences appear near and at the extremality limit.

As the general $\langle T_a^b\rangle^{ABG}$ contains terms that are quadratic and cubic in η, the case of arbitrary coupling is more complicated. Again, for small and intermediate values of q there is a similarity between the $\langle T_a^b\rangle$ evaluated for the minimally coupled scalar field in the ABG geometry and its RN counterpart. Modifications for q slightly exceeding 0.8, which are mainly due to the term $T_a^{(2)b}$, are noticeable although there are still some similarities. Comparison of $\langle T_a^b\rangle^{ABG}$ for charges close to q_{extr} indicates that the radial dependences for both couplings are completely different. Indeed, the behavior of the stress-energy tensor for the minimal coupling is far more complicated as compared with its almost monotonic radial dependence for $\eta=0$. Moreover, the former is even more sensitive to changes of q, especially near the extremality limit. In addition, new features occur, such as, for example, positivity of the energy density at the event horizon for certain values of q.

It should be emphasized that, being local, the Schwinger-DeWitt approximation does not describe particle creation, and, therefore, it must not be applied in strong or rapidly varying gravitational fields. However, it is expected that for sufficiently massive fields the method will provide a good approximation of the exact renormalized stress-energy tensor.

Finally, we remark that, although complicated, the derived stress-energy tensor may be employed as a source term of the semiclassical Einstein field equations. Indeed, preliminary calculations indicate that it is possible to find an analytical perturbative solution to the back reaction, and what makes this issue even more interesting and worth further studies is the regularity of the geometry of the ABG black hole. We intend to return to this group of problems elsewhere.

[1] B.A. Taylor, W.A. Hiscock, and P.R. Anderson, Phys. Rev. D **61**, 084021 (2000).
[2] J.W. York, Phys. Rev. D **31**, 775 (1985).
[3] C.O. Lousto and N. Sanchez, Phys. Lett. B **212**, 411 (1988).
[4] D. Hochberg and T.W. Kephart, Phys. Rev. D **47**, 1465 (1993).
[5] D. Hochberg, T.W. Kephart, and J.W. York, Phys. Rev. D **48**, 479 (1993).
[6] D. Hochberg, T.W. Kephart, and J.W. York, Phys. Rev. D **49**, 5257 (1994).
[7] P.R. Anderson, W.A. Hiscock, J. Whitesell, and J.W. York, Phys. Rev. D **50**, 6427 (1994).
[8] J. Matyjasek, Acta Phys. Pol. B **29**, 529 (1998).
[9] V.P. Frolov and A.I. Zel'nikov, Phys. Lett. **115B**, 372 (1982).
[10] V.P. Frolov and A.I. Zel'nikov, Phys. Lett. **123B**, 197 (1983).
[11] V.P. Frolov and A.I. Zelnikov, Phys. Rev. D **29**, 1057 (1984).
[12] I.G. Avramidi, Ph.D. thesis, Moscow State University, hep-th/9510140.
[13] I.G. Avramidi, Theor. Math. Phys. **79**, 494 (1989).
[14] I.G. Avramidi, Nucl. Phys. **B355**, 712 (1991).
[15] J. Matyjasek, Phys. Rev. D **61**, 124019 (2000).
[16] J. Matyjasek, Phys. Rev. D **63**, 084004 (2001).
[17] P.R. Anderson, W.A. Hiscock, and D.A. Samuel, Phys. Rev. D **51**, 4337 (1995).
[18] B.A. Taylor, W.A. Hiscock, and P.R. Anderson, Phys. Rev. D **55**, 6116 (1997).
[19] K.A. Bronnikov, V.N. Melnikov, G.N. Shikin, and K.P. Stanukowicz, Ann. Phys. (N.Y.) **118**, 84 (1979).
[20] E. Ayón-Beato and A. García, Phys. Lett. B **464**, 25 (1999).
[21] K.A. Bronnikov, Phys. Rev. D **63**, 044005 (2001).
[22] A. Burinskii and S.R. Hildebrandt, Phys. Rev. D **65**, 104017 (2002).
[23] I.H. Salazar, A. Garcia, and J. Plebanski, J. Math. Phys. **28**, 2171 (1987).
[24] K.A. Bronnikov, Phys. Rev. Lett. **85**, 4641 (2000).
[25] M. Novello, S.E. Perez Bergliaffa, and J.S. Salim, Class. Quantum Grav. **17**, 3821 (2000).
[26] M. Novello, V.A. De Lorenci, J.S. Salim, and R. Klippert, Phys. Rev. D **61**, 045001 (2000).
[27] M. Novello, S.E. Perez Bergliaffa, and J.S. Salim, Phys. Rev. D **63**, 083511 (2001).
[28] R.M. Corless *et al.*, Adv. Comput. Math. **5**, 329 (1996).